



This is a repository copy of *The origin and evolution of magnetic white dwarfs in close binary stars*.

White Rose Research Online URL for this paper:
<https://eprints.whiterose.ac.uk/173667/>

Version: Accepted Version

Article:

Schreiber, M.R., Belloni, D., Gänsicke, B.T. et al. (2 more authors) (2021) The origin and evolution of magnetic white dwarfs in close binary stars. *Nature Astronomy*, 5 (7). pp. 648-654.

<https://doi.org/10.1038/s41550-021-01346-8>

This is a post-peer-review, pre-copyedit version of an article published in *Nature Astronomy*. The final authenticated version is available online at:
<https://doi.org/10.1038/s41550-021-01346-8>.

Reuse

Items deposited in White Rose Research Online are protected by copyright, with all rights reserved unless indicated otherwise. They may be downloaded and/or printed for private study, or other acts as permitted by national copyright laws. The publisher or other rights holders may allow further reproduction and re-use of the full text version. This is indicated by the licence information on the White Rose Research Online record for the item.

Takedown

If you consider content in White Rose Research Online to be in breach of UK law, please notify us by emailing eprints@whiterose.ac.uk including the URL of the record and the reason for the withdrawal request.



eprints@whiterose.ac.uk
<https://eprints.whiterose.ac.uk/>

The origin and evolution of magnetic white dwarfs in close binary stars

Matthias R. Schreiber^{1,2,*}, Diogo Belloni^{3,1,*}, Boris T. Gänsicke⁴, Steven G. Parsons⁵, Monica Zorotovic⁶

¹*Departamento de Física, Universidad Técnica Federico Santa María, Av. España 1680, Valparaíso, Chile*

²*Millennium Nucleus for Planet Formation (NPF), Valparaíso, Chile*

³*National Institute for Space Research, Av. dos Astronautas, 1758, 12227-010, São José dos Campos, SP, Brazil*

⁴*Department of Physics, University of Warwick, Coventry CV4 7AL, UK*

⁵*Department of Physics and Astronomy, University of Sheffield, Sheffield S3 7RH, UK*

⁶*Instituto de Física y Astronomía, Universidad de Valparaíso, Av. Gran Bretaña 1111, Valparaíso, Chile*

**These authors contributed equally to this work*

The origin of magnetic fields in white dwarfs remains a fundamental unresolved problem in stellar astrophysics. In particular, the very different fractions of strongly ($\gtrsim 1$ MG) magnetic white dwarfs in evolutionarily linked populations of close white dwarf binary stars cannot be reproduced by any scenario suggested so far. Strongly magnetic white dwarfs are absent among detached white dwarf binary stars that are younger than approximately 1 Gyr. In contrast, in semi-detached cataclysmic variables in which the white dwarf accretes from a

low-mass star companion, more than one third host a strongly magnetic white dwarf¹. Here we present binary star evolutionary models that include the spin evolution of accreting white dwarfs and crystallization of their cores, as well as magnetic field interactions between both stars. We show that a crystallization- and rotation-driven dynamo similar to those working in planets and low-mass stars² can generate strong magnetic fields in the white dwarfs in cataclysmic variables which explains their large fraction among the observed population. When the magnetic field generated in the white dwarfs connects with that of the secondary stars, synchronization torques and reduced angular momentum loss cause the binary to detach for a relatively short period of time. The few known strongly magnetic white dwarfs in detached binaries, including AR Sco³, are in this detached phase.

The vast majority of close binary stars containing at least one white dwarf form through common envelope evolution⁴. The emerging detached post common envelope binary stars evolve towards shorter orbital periods driven by angular momentum loss⁵ and eventually become semi-detached cataclysmic variable stars (CVs)⁶. Despite this clear evolutionary link, the fraction of strongly magnetic white dwarfs differs drastically between both types of close white dwarf binaries.

We know more than 160 CVs with a strongly (larger than 1 MG) magnetic white dwarf⁷. In most of these systems the white dwarf accretes from its Roche-lobe filling low-mass star companion along the magnetic field lines. Due to interactions of the magnetic fields of both stars, the rotation of the white dwarf is synchronised with the orbital motion of the secondary star, such systems are called *polars*. In a smaller but still important fraction of CVs, the magnetic field of the

white dwarf disrupts the inner parts of the accretion disk but the magnetic fields of both stars do not connect. In these so-called *intermediate polars* the rotation of the white dwarf and the orbital motion are therefore not synchronised⁸. A recent study of a volume-limited sample has shown that over a third of all CVs contain a magnetic white dwarf, with polars and intermediate polars making up approximately 29 and 7 per cent of the total population¹.

The situation is very different among the detached systems that are believed to be the progenitors of CVs. Only 15 strongly magnetic white dwarfs in close detached binaries are currently known^{9,10} and they make up less than two per cent of the over one thousand known systems^{11,12}. All but one of these detached magnetic white dwarf binaries have been identified due to a peculiar emission line¹³, which turned out to be the third harmonic of a cyclotron fundamental emitted by a low-density plasma. This observational finding is convincingly interpreted as resulting from wind accretion onto a strongly magnetic white dwarf in a close but detached binary¹⁴. Because angular momentum loss will eventually drive them into a semi-detached CV configuration, these systems have been termed *pre-polars*⁹. The only exception is AR Sco, which was discovered because of the optical and radio pulses of its rapidly (1.97 min) rotating white dwarf³. AR Sco and most pre-polars are located in the orbital period range between 3 and 5 hours, their secondary stars are close to filling their Roche-lobes (R/R_L typically exceeding 80 per cent)¹⁰, and the magnetic white dwarfs are cold with effective temperatures typically below 10,000 K which implies that they formed at least one Gyr ago. Among younger close detached white dwarf binaries, not a single strongly magnetic white dwarf has been found^{15,16}. This puzzling situation, a large fraction (approximately 35 per cent) of strongly magnetic white dwarfs in CVs and the much smaller fraction

of magnetic white dwarfs among the detached systems that are believed to be CV progenitors, was aptly expressed by Liebert¹⁵ who asked *Where Are the Magnetic White Dwarfs with Detached, Non-degenerate Companions?* This fundamental question of stellar evolution has remained without an answer for 15 years and the solution must link the evolution of white dwarf binaries and magnetic field generation in white dwarfs.

Several hypotheses have been put forward to explain magnetic field generation in white dwarfs in the last decades. In their present form, the fossil field scenario¹⁷, a dynamo operating during common envelope evolution¹⁸, or coalescing double white dwarfs¹⁹ face one serious problem when considered as the main formation mechanism for close magnetic white dwarf binaries. In all these cases the magnetic fields are generated during the formation process of the white dwarf, i.e. according to the current versions of these theories also detached post common envelope binaries containing hot white dwarfs should host strong magnetic fields which is clearly not the case¹⁶.

As the only mechanism that depends on the age of the white dwarf, a dynamo similar to those operating in low-mass main-sequence stars and planets² has been suggested to operate if the white dwarf is rotating rapidly when the core of the white dwarf is crystallizing²⁰. As a white dwarf with a Carbon/Oxygen core cools, the ions in the core begin to freeze in a lattice structure. During crystallization the chemical potential, temperature, and pressure of the liquid and solid phases must remain equal. As a consequence, in crystallizing white dwarfs the solid phase becomes richer in oxygen and sinks while the carbon excess mixes with the outer liquid envelope which

is redistributed by Rayleigh–Taylor instabilities. This configuration is similar to that found in the core of the Earth, where the light element release associated with the inner core growth is a primary driver of the dynamo generating the Earth’s magnetic field²¹.

The predicted field strengths generated by this dynamo in white dwarfs depend entirely on the scaling law that is assumed. Applying the same scaling law that is used for planetary magnetic fields leads to field strengths in white dwarfs of up to approximately 1 MG²⁰. However, taking into account a likely dependence of the dynamo efficiency on the magnetic Prandtl number and that in white dwarfs this number is orders of magnitudes larger than in planets, one could expect this dynamo to be able to generate fields much stronger than 1 MG (for more details see Methods).

Assuming that the crystallization and rotation driven dynamo can generate strong magnetic fields we computed evolutionary tracks starting with non-magnetic post common envelope binaries. We incorporated several physical mechanisms in the stellar evolution code MESA²². The spin-up of the white dwarf due to the accretion of angular momentum²³ was included as well as crystallization of the white dwarf²⁴. We furthermore incorporated the reduction in angular momentum loss through magnetic braking when the magnetic fields of both stars connect²⁵, a condition for synchronisation²⁶, and a prescription for angular momentum transfer from the spin of the white dwarf to the orbit during synchronisation (see Methods for more details).

Figure 1 shows an exemplary evolutionary track resulting from our simulations and a schematic illustration of the different stages the system passes through. In our model the white dwarf is born without a strong magnetic field which is in agreement with the absence of strongly magnetic white

dwarfs in young close detached post common envelope binaries (stage 1). The non-magnetic detached binary star then evolves slowly towards shorter orbital periods and the white dwarf cools. When the secondary fills its Roche-lobe the binary becomes a CV, accretion spins up the white dwarf²³ and the core may be crystallizing (stage 2). If this happens, both conditions for the crystallization and rotation driven dynamo are met and a strong magnetic field is generated (stage 3). If the magnetic field is strong enough to connect with the field of the secondary star the latter provides a synchronising torque on the white dwarf spin. The spin angular momentum transferred to the orbital motion due to the synchronising torque causes the secondary to detach from its Roche-lobe. This effect is supported by the fact that the connection of the two magnetospheres reduces angular momentum loss due to magnetic wind braking because part of the gas escaping from the secondary is accreted by the white dwarf along the connected field lines, instead of leaving the system²⁵. At the beginning of synchronisation the system becomes a radio pulsing white dwarf binary, such as AR Sco, in which a rapidly rotating white dwarf spins down on a relatively short time scale (stage 4) of approximately 1 – 10 Myr. When the white dwarf spin is synchronised with the orbital motion of the secondary star, the binary star has evolved into the pre-polar stage in which wind accretion generates the observed cyclotron emission (stage 5). Angular momentum loss through reduced magnetic braking and gravitational radiation brings the stars closer together until the secondary again fills its Roche-lobe and finally a polar is formed (stage 6). The detached phase (stage 3-5) occurs preferentially for orbital periods shorter than roughly 5 hr as the reduction of magnetic braking and the transfer of spin angular momentum to the orbit have less impact at longer periods. Detached phases occur less frequently at orbital periods shorter than approximately 3 hr because

the conditions for magnetic field generation are typically met at early stages of CV evolution (see Methods for a detailed comparison of observations and model predictions).

While a different mechanism such as common envelope merger¹⁸ and/or double white dwarf merger¹⁹ is probably required to explain most single white dwarfs with magnetic field strengths exceeding 1 MG (see Supplementary Material for details), the new evolutionary sequence predicted by our model is in excellent agreement with the observations of close binary stars containing strongly magnetic white dwarfs. As the conditions for the dynamo are relatively frequently met in CVs (see Supplementary Material for a discussion of the predicted relative numbers), our model successfully reproduces the large fraction of CVs containing magnetic white dwarfs. The few known detached binaries containing magnetic white dwarfs are not progenitors of CVs but instead systems that have been non-magnetic CVs in the past and where mass transfer stopped because the field was generated. This naturally explains why there is not one single hot and young strongly magnetic white dwarf in a detached binary. Instead our model predicts that all of them are older than 1 Gyr with crystallizing cores as is observed (Fig. 2) and also explains why all 15 currently known close detached binaries containing magnetic white dwarfs are close to Roche-lobe filling (Supplementary Figure 1). Furthermore, the observed clustering of pre-polars in the orbital period range of 3 – 5 hr is well reproduced in our simulations as the detached phase typically occurs in this range. Finally, our evolutionary sequence predicts short phases of rapidly rotating and strongly magnetic white dwarfs in detached binaries thereby offering an explanation for the existence of the radio pulsating system AR Sco. We conclude that a dynamo-driven generation of magnetic fields in white dwarfs resolves several long standing problems at once.

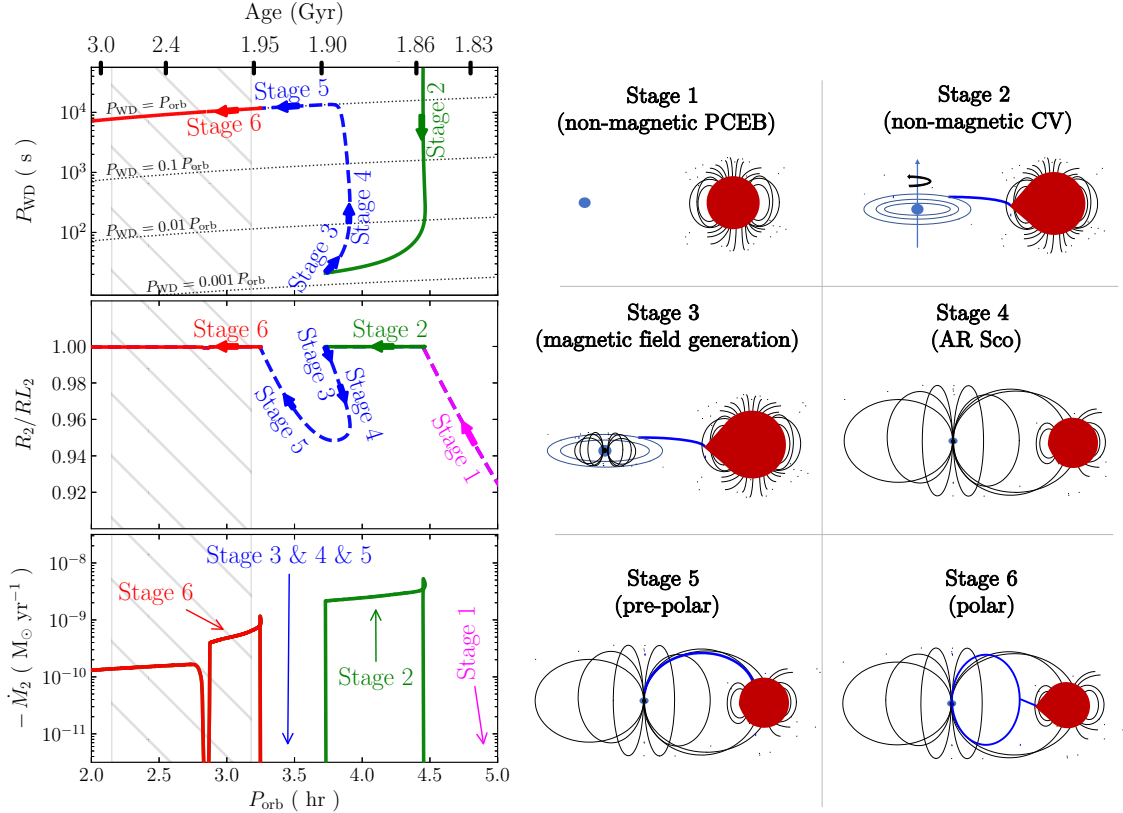


Fig. 1. Spin period, Roche-lobe filling factor, and mass transfer rate as a function of orbital period.

The slowly rotating white dwarf (stage 1) in a non-magnetic post common envelope binary is spun-up due to accretion (stage 2). In case the white dwarf is crystallizing a strong magnetic field is generated by a dynamo (stage 3) and as soon as it connects with the field of the secondary the system becomes detached. At first it resembles the radio pulsing white dwarf binary AR Sco (stage 4). When the spin of the white dwarf and the orbital motion are synchronised (stage 5) the system becomes a pre-polar before mass transfer starts again (stage 6). When the secondary becomes fully convective, a second short detached phase (between ≈ 2.07 and ≈ 2.09 Gyr) occurs which represents a short version of the classical orbital period gap (hatched region).

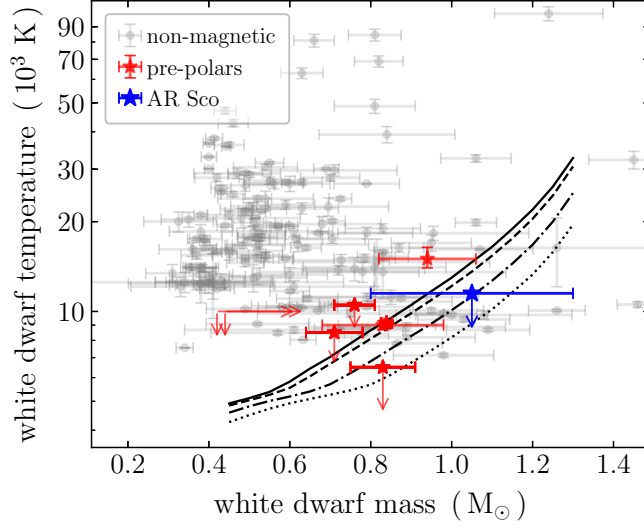


Fig. 2 Observed white dwarf effective temperatures versus their masses for non-magnetic post common envelope binaries from the Sloan Digital Sky Survey (light gray)^{12,27}, pre-polars (red)¹⁰, and the first radio pulsing white dwarf binary AR Sco (blue)^{3,28}. The errors on the observations correspond to 1σ and arrows indicate upper limits. The lines represent the mass fraction of crystallized matter in the white dwarf interiors. Solid, dashed, dash-dotted and dotted lines show the temperature for each white dwarf mass corresponding to the onset of crystallization, 10 per cent of mass is crystallized, 50 per cent and 80 per cent, respectively²⁴. As predicted by our scenario, magnetic systems host on average much older and more massive white dwarfs than their non-magnetic counterparts. The trend towards larger masses in magnetic systems is totally consistent with the observed white dwarf mass distribution in cataclysmic variables^{29,30} which fits with the model prediction that these systems have been CVs in the past. In addition, the white dwarfs in AR Sco and all pre-polars are consistent with having crystallizing cores.

Methods

The convective dynamo and scaling laws. The magnetic fields of Earth and Jupiter, as well as those of rapidly rotating low-mass stars, are generated by convection-driven dynamos. The basic ingredients for these dynamos to work are a strong density stratification, and an extended convection zone. To derive the magnetic field strength from fundamental properties of a given planet or star the use of scaling laws is required. In general it is neither clear which quantities need to be considered in these scaling laws nor whether a single scaling law exists for all planets and stars whose magnetic fields are generated by the convective dynamo. In the last decades, several scaling laws have been proposed, most of them based on the assumption of a balance between Coriolis force and Lorentz force³¹. In recent years a scaling law derived from geo-dynamo models³² which assumes the energy flux to be the dominant parameter has become popular. This scaling law has been shown to successfully explain the field strengths of Earth and Jupiter as well as those of rapidly rotating fully convective stars².

In the first application of the convective dynamo mechanism to white dwarfs this energy flux scaling law was assumed²⁰. The vast majority of white dwarfs consist of Carbon and Oxygen. As a white dwarf cools, the ions in the core begin to freeze in a lattice structure³³. The phase diagram of the carbon–oxygen mixture is of the spindle form^{34,35}, therefore, as soon as the white dwarf has sufficiently cooled and starts to crystallize, the solid phase becomes richer in oxygen and sinks while the carbon excess mixes with the outer liquid envelope. As a consequence, an oxygen-rich core forms which is significantly denser than the carbon-rich liquid which is redistributed

by the Rayleigh–Taylor instability^{36,37}. Such a strong density stratification in combination with convection represent the key ingredients for the dynamo generating the Earth’s magnetic fields and those of low-mass stars. Assuming the same scaling law that has been successfully applied to the Earth, Jupiter, and rapidly rotating fully convective stars for crystallizing white dwarfs predicts field strengths of at most a few MG²⁰ which, if true, would exclude the dynamo from being the mechanism generating the much stronger 1 – 200 MG fields found in white dwarfs in close binary stars.

Here we argue that this scaling law is most likely not applicable to white dwarfs. In the magneto hydrodynamic simulations that led to the energy flux scaling law, the magnetic Prandtl number (P_m , defined as the ratio between viscous and magnetic diffusivity) is assumed to be equal to one. However, in both fully convective stars as well as the Earth this number is significantly smaller ($10^{-4} - 10^{-5}$ and 10^{-6} , respectively). To quote the discovery paper³² of the energy flux scaling law “*we cannot rule out an additional dependence on other parameters, in particular the magnetic Prandtl number. Although the suggested dependence is weak, it poses a serious problem. Given the large range of extrapolation over five orders of magnitude from our models to planetary values of P_m , the results obtained from the scaling laws with or without a dependence on P_m differ substantially.*” This early statement has been confirmed more recently by Brandenburg³⁸ who wrote: “*This leads to a scaling law that has been verified over many orders of magnitude (Christensen et al. 2009). As we have seen, this scaling law must be affected by P_m ...*”. Given that the magnetic Prandtl number for crystallizing white dwarfs has been estimated to be 0.58^{20} , i.e. roughly six orders of magnitude larger than that of the Earth and still 4 – 5 orders of magnitude

larger than that of fully convective low-mass stars, the dynamo could be more efficient in white dwarfs.

In fact, the comparison between predicted and observed field strengths of single white dwarfs presented by Isern et al.²⁰ indeed indicates that observed fields in crystallizing single white dwarfs exceed those predicted by the energy flux scaling law. The energy flux scaling law is only applicable in the saturated regime of the dynamo, i.e. it only works for rapidly rotating objects with Rossby numbers below ~ 0.1 . For white dwarfs, this implies spin periods shorter than $\sim 90 \text{ s}^{20}$. In white dwarfs that rotate substantially slower, the generated fields should be smaller than those predicted by the energy flux scaling law. All the observed magnetic single white dwarfs within 20 pc (Table 1 of Isern et al.²⁰) rotate with periods ranging from hours to days. Despite rotating orders of magnitudes too slow for the energy flux scaling law to be applicable (which is applicable in the saturated regime), the field strengths of these white dwarfs even slightly exceed those predicted by the energy flux scaling law. This implies that, if a convection driven dynamo works in crystallizing and rotating white dwarfs, the energy flux scaling law underestimates the field strengths of slowly rotating single white dwarfs. The field strengths of rapidly rotating white dwarfs in the saturated regime should therefore as well largely exceed those predicted by the energy flux scaling law. A suitably revised scaling law that incorporates the dependence on the magnetic Prandtl number is therefore likely to predict fields much stronger than $\sim 1 \text{ MG}$ for white dwarfs that rotate in the saturated regime of the dynamo.

Based on the above arguments, we here assumed that a rapidly rotating white dwarf ($P_{\text{WD}} \simeq$

20 – 30 s) with a fractional crystallized mass between 10 and 80 percent can drive a dynamo that generates the large magnetic field strengths observed in white dwarfs in cataclysmic variables (up to several 100 MG). We calculate the evolution of close detached white dwarf binaries and cataclysmic variables (CVs) using MESA²², taking into account the spin-up due to accretion and crystallization due to cooling of the white dwarf as well as magnetic field generation if a crystallizing white dwarf rotates rapidly.

Spin-up of the white dwarf. If a white dwarf accretes from an accretion disk in a CV its angular momentum and therefore its angular velocity increases, while during nova eruptions the white dwarf loses mass and angular momentum. According to King et al.²³, the resulting angular momentum balance for an accreting white dwarf is given by

$$I \frac{d\omega}{dt} = \alpha (-\dot{M}_2) (G M_{\text{WD}} R_{\text{WD}})^{1/2} + (1 + \epsilon) (\dot{M}_2 \eta R_{\text{WD}}^2 \omega), \quad (1)$$

where ω is the white dwarf spin, I its moment of inertia, G the gravitational constant, \dot{M}_2 the mass transfer rate averaged over nova cycles, and M_{WD} and R_{WD} are the white dwarf mass and radius.

The first term in the right-hand part of the equation corresponds to the spin-up due to accretion, while the second term represents the spin-down due to material leaving the white dwarf during nova eruptions. The parameter $0 \leq \alpha \leq 1$ represents the spin-up efficiency, which might be smaller than one due to mass loss processes not considered in equation Eq. 1 (e.g. winds from the inner accretion disk or jets from the boundary layer/white dwarf). The parameter $0 \leq \epsilon = \dot{M}_{\text{WD}}/\dot{M}_2 \leq 1$ relates the mass loss of the white dwarf to the mass transfer rate. The range of possible values reflects the fact that the white dwarf mass might decrease over a nova cycle, i.e. more mass

might be expelled during a nova eruption than was accreted between two eruptions. The parameter $0 \leq \eta \leq 1$ represents the square of the radius of gyration of the ejected envelope and depends on the geometry of nova eruptions.

By solving the non-homogeneous differential equation 1, the WD spin as a function of the donor mass is given by

$$\omega = \frac{C_1}{C_2} + C_3 \exp (C_2 M_2) , \quad (2)$$

where M_2 is the donor mass in solar masses and the terms C_1 , C_2 and C_3 are given by

$$C_1 = \alpha \frac{A}{k^2} \frac{\omega_{\text{bk},0}}{M_{\text{WD},0}} \quad (3)$$

$$C_2 = \frac{\eta}{k^2 M_{\text{WD}}} (1 + \varepsilon) + B \varepsilon \quad (4)$$

$$C_3 = \left(\omega_0 - \frac{C_1}{C_2} \right) \exp (-C_2 M_{2,0}) \quad (5)$$

where ω_{bk} is the break-up white dwarf spin, given by

$$\omega_{\text{bk}} = \sqrt{\frac{GM_{\text{WD}}}{R_{\text{WD}}^3}} = 2 \pi \sqrt{\left(\frac{M_{\text{WD}}}{M_{\odot}}\right) \left(\frac{R_{\text{WD}}}{\text{au}}\right)^{-3}} \text{ yr}^{-1} . \quad (6)$$

The moment of inertia I is $k^2 M_{\text{WD}} R_{\text{WD}}^2$, with k given by $0.452 + 0.0853 \log_{10} (1 - M_{\text{WD}}/1.44M_{\odot})$,

if $M_{\text{WD}} \lesssim 1.368 M_{\odot}$, and ≈ 0.275 , if $M_{\text{WD}} \gtrsim 1.368 M_{\odot}$. The constants A and B are given by

$$A = \left[\frac{1 - 0.61 (M_{\text{WD},0}/M_{\odot})^{4/3}}{1 - 0.61 (M_{\text{WD}}/M_{\odot})^{4/3}} \right]^{3/4} , \quad (7)$$

$$B = \frac{3.05 (M_{\text{WD}}/M_{\odot})^{4/3} - 1}{3 [1 - 0.61 (M_{\text{WD}}/M_{\odot})^{4/3}]} + \frac{0.051 (M_{\text{WD}}/M_{\odot})}{k [1 - 0.69 (M_{\text{WD}}/M_{\odot})]} . \quad (8)$$

The sub-index 0 in some quantities indicates their initial values just after the common-envelope evolution.

Synchronisation of the white dwarf. In accreting high-field magnetic white dwarf binaries the magnetic field dominates the accretion process. For sufficiently strong white dwarf magnetic moments, the overflowing material is channelled along the white dwarf's magnetic field lines as soon as the magnetic pressure dominates the gas ram pressure. For such strong white dwarf magnetic fields, the interaction of the magnetospheres of the white dwarf and the donor cause a synchronizing torque on the white dwarf³⁹.

We assume here that the onset of synchronization occurs when the synchronizing torque is greater than the accretion torque (assuming that the magnetospheres of the white dwarf and the donor are connected)²⁶, i.e.

$$\frac{\mu_{\text{WD}}}{10^{33} \text{ G cm}^3} > 1.11 \left(\frac{-\dot{M}_2}{10^{16} \text{ g/s}} \right) \left(\frac{M_{\text{tot}}}{M_{\odot}} \right)^{1/3} \left(\frac{M_2}{M_{\odot}} \right)^{-1} \left(\frac{P_{\text{orb}}}{\text{hr}} \right)^{1/3} \left(\frac{B_2}{100 \text{ G}} \right)^{-1} \left[0.5 - 0.277 \log_{10} \left(\frac{M_2}{M_{\text{WD}}} \right) \right]^2 \quad (9)$$

where μ_{WD} is the white dwarf magnetic moment, M_2 is the donor mass, $M_{\text{tot}} = M_{\text{WD}} + M_2$ is the binary total mass, P_{orb} is the orbital period and B_2 is the strength of the magnetic field of the secondary star.

Once the condition provided by Equation 9 is satisfied, the spin-down process starts. For simplicity, we assume that the white dwarf spin decreases exponentially on a given time-scale, i.e.

$$\omega(t) = \Omega + C e^{-t/\tau} \quad (10)$$

where τ is the synchronisation time-scale, Ω the orbital angular velocity, ω the WD spin, and $C = \omega_0 - \Omega$ is a constant (because variations in Ω are negligible during the spin-down phase).

This assumption gives

$$\frac{d\omega}{dt} = \frac{(\Omega - \omega)}{\tau}. \quad (11)$$

This equation of course represents a very crude approximation of a very complicated process. The torque on the primary as a function of asynchronism has been calculated previously in great detail⁴⁰, but only for rather small asynchronism. Performing such detailed calculations of the magnetic field interaction for the large asynchronism in our systems, is beyond the scope of this paper. For the purpose of this paper, we assume that the total angular momentum loss by the white dwarf is transferred to the secondary, incorporated in the orbital motion, and that this occurs on the time-scale τ , i.e.

$$\dot{J}_{\text{orb}} = -\frac{d}{dt}(\omega I) = I \frac{(\omega - \Omega)}{\tau} > 0. \quad (12)$$

In this simple model the torque is always decreasing with increasing synchronism which might not be correct⁴⁰. However, this should not affect the validity of our model as only the amount of spin angular momentum transferred to the orbit and the time scale on which this happen are important for the secular evolution of a given system.

Reduced magnetic braking. For secondary stars still containing a radiative core, angular momentum loss through magnetic wind braking drives mass transfer in CVs^{6,11}. The strength of magnetic braking depends significantly on the extension of wind zones compared to dead zones. The latter correspond to regions where gas is prevented from escaping the star due to the pressure of closed magnetic field loops, i.e. the magnetic pressure is greater than the thermal pressure⁴¹. If the white dwarf in a CV is strongly magnetic and the magnetospheres of both stars connect, the wind zone is reduced which leads to a decrease of orbital angular momentum loss due to magnetic braking^{42,43}.

For short orbital periods and/or strong magnetic fields, angular momentum loss through magnetic braking can be completely suppressed.

The reduction of magnetic braking for a given μ_{WD} can be parametrized with the fraction of open field lines (Φ). In the extreme case of no wind zone, i.e. μ_{WD} is strong enough to prevent any magnetic braking, $\Phi = 0.0$. On the other hand, in case the impact of the magnetic moment is negligible, the second dead zone does not exist and magnetic braking is not reduced, leading to $\Phi = 0.258$. This prescription for the reduction of MB depends on the binary parameters and μ_{WD} , and therefore allows us to incorporate the impact of strong WD magnetic fields in binary evolution codes^{42,25}.

The resulting angular momentum loss due to magnetic braking in the presence of a strongly magnetic white dwarf ($\dot{J}_{\text{MB,mag}}$) can be written as

$$\dot{J}_{\text{MB,mag}} = \dot{J}_{\text{MB,non-mag}} \left(\frac{\Phi}{0.258} \right)^{5/3}, \quad (13)$$

where $\dot{J}_{\text{MB,non-mag}}$ is the angular momentum loss due to magnetic braking in non-magnetic CVs.

In this work we used the widely adopted RVJ prescription⁴⁴, with $\gamma = 3$, i.e.

$$\dot{J}_{\text{MB,non-mag}} = -3.8 \times 10^{-30} \left(\frac{M_2}{g} \right) R_{\odot}^4 \left(\frac{R_2}{R_{\odot}} \right)^3 \left(\frac{\Omega_2}{\text{s}^{-1}} \right)^3, \quad (14)$$

where R_2 is the donor radius and Ω_2 is the donor spin, which is the same as the orbital angular velocity. This reduced magnetic braking model has been incorporated in binary population models of magnetic CVs and has been shown to convincingly reproduce the orbital period distribution of magnetic CVs²⁵ and we here implemented the same prescription in MESA.

Modelling magnetic CV evolution with MESA. The above described effects were incorporated in the stellar evolution code Modules for Experiments in Stellar Astrophysics (MESA) (version r10108)^{45–48,22}. The MESA equation of state is a blend of the OPAL⁴⁹, SCVH⁵⁰, PTEH⁵¹, HELM⁵², and PC⁵³ equation of states. Radiative opacities are primarily from OPAL^{54,55}, being the regime low-temperature dominated⁵⁶ or high-temperature, Compton-scattering dominated⁵⁷. Electron conduction opacities are also included⁵⁸. Nuclear reaction rates are a combination of rates from NACRE⁵⁹, JINA REACLIB⁶⁰, plus additional tabulated weak reaction rates^{61–63}. Screening is included⁶⁴ as well as thermal neutrino loss⁶⁵. Roche lobe radii in binary systems are computed using Eggleton’s fit⁶⁶ and mass transfer rates in Roche lobe overflowing binary systems are determined following Ritter’s prescription⁶⁷.

The parameters of our standard model were set as follows. During the whole CV evolution we assumed that all material accreted by the WD is lost through nova eruptions. In Equation 1, this corresponds to setting $\epsilon = 0$. For the geometry of nova shells, we assumed that mass leaves the WD with some asymmetry (i.e. neither completely spherical nor radial), which implies values of η in Eq. 1 between $2/3$ and 1 . We set $\eta = 2.5/3$. Additional mass loss from the system^{68,69} was taken into account by using $\alpha = 0.75$ in Equation 1. The donor magnetic field was assumed to be $B_2 = 1$ kG, which is consistent with recent measurements of field strengths of low-mass stars⁷⁰. We fixed the WD mass to $0.8 M_\odot$, which corresponds to the average value found among observed CVs^{29,71}. For the white dwarf magnetic field, we assume $B_{\text{WD}} = 60$ MG, which is slightly stronger than the average field strength of polars⁷, but corresponds to the average field strength found in pre-polars⁹. We assumed that the dynamo is efficient only if the core of the

white dwarf is crystallizing (between 10 and 80 per cent crystallized) and the spin period of the white dwarf is $\simeq 20 - 30$ s. Finally, for the synchronisation time-scale, we set $\tau = 1$ Myr, which is consistent with the expected rapid spin-down in close binaries harbouring a rapidly rotating magnetic white dwarf such as AR Sco³.

Using this set of parameters our model can reproduce the observations of magnetic detached and semi-detached close white dwarf binary stars (Supplementary Figure 1). According to this model, pre-polars and AR Sco have been CVs in the past and at that time the strong magnetic fields of their white dwarfs were generated. This prediction is in perfect agreement with the cool white dwarf temperatures of these detached systems, with them being close to Roche-lobe filling, and with their preferred occurrence in the 3-5 hr orbital period range.

We emphasise that no fine-tuning was required to obtain this agreement. In contrast, the model naturally explains the observations and variations of the key parameters do not affect the general predictions (Supplementary Figures 2, 3 and 4). For instance, by changing the spin-up parameters (i.e. α , η and ϵ), the only effect is to accelerate or delay the spin-up of the white dwarf and slightly change the minimum spin period that can be reached²³. For all reasonable values of these parameters the white dwarf will manage to spin-up to sufficiently large spin rates so that the conditions for generating strong magnetic fields can eventually be met.

Similarly, varying the synchronisation time-scale τ affects the synchronising torque but does not change the evolutionary sequence (Supplementary Figure 2). The shorter τ , the stronger the spin-down torque and therefore the longer the detached phase. Only for $\tau \gtrsim 100$ Myr, the detached

phase can be fully prevented if, in addition, the magnetic field strength of the white dwarf does not exceed ~ 200 MG. The latter condition arises as for very strong fields reduced magnetic braking alone can cause the system to detach in full analogy to the mechanism producing the classic orbital period gap.

A slightly stronger constraint on the synchronisation time scale results from the fact that it should not exceed the duration of the generated detached phase as otherwise the observed synchronised pre-polars would remain unexplained. For white dwarfs rotating near break-up, in order to have a synchronised system after the detached phase, time scales cannot exceed 30 – 40 Myr. This maximum time scale is definitely not a problem for our model, since the synchronisation time scales for the range of magnetic field strengths we consider here, i.e. those of polars, pre-polars and AR Sco, are expected to be well below 30 – 40 Myr⁷².

The overall evolution does also not sensitively depend on the assumed white dwarf and secondary star magnetic fields. Varying these field strengths changes only slightly the condition for synchronisation (Equation 9). For weaker/stronger B_2 , this condition becomes more/less restrictive. Increasing or decreasing B_{WD} affects somewhat the orbital period at which synchronism can be obtained, which is longer for stronger fields (Supplementary Figure 3). The white dwarf magnetic field strengths also affects the duration of the detached phase. The stronger the white dwarf magnetic field, the more angular momentum loss due to magnetic braking is reduced and the longer it takes the system to evolve back into a semi-detached configuration.

The largest and most critical assumption in our model certainly are the conditions we assume

for magnetic field generation which represent a strong but reasonable simplification. According to the most popular scaling law, the dynamo saturates for fast rotation (in white dwarfs for spin periods below 90 s^{20}) and the produced field strength depends then solely on the convective energy flux. However, as outlined above, the efficiency of the dynamo is also expected to significantly depend on the magnetic Prandtl number which is not considered in any currently available scaling law. As long as a reliable scaling law taking into account this dependency is not available, describing the evolution of close magnetic white dwarf binaries needs to be based on simple assumptions such as those made in this paper. As soon as realistic scaling laws for the dynamo operating in crystallizing white dwarfs are available, we plan to incorporate those together with detailed white dwarf models into our simulations.

The aim of this paper is to show how the evolution of close white dwarf binaries is affected if, and that is a reasonable assumption, crystallization and fast rotation can generate a strong magnetic field. We would expect the generated field strength in these models to depend on the rotation rate and the energy flux in the convection zone. Given the large range of orbital periods at the end of common envelope evolution, and the therefore large variety of evolutionary time scales towards the CV phase, we expect that such a more detailed model can explain the large range of field strength observed in magnetic CVs including those of intermediate polars. In case of the latter the field is simply not strong enough to synchronise the white dwarf spin with the orbital motion and the system does not enter a detached phase apart from the usual 2 – 3 hr orbital period gap.

In the Supplementary Information we present a detailed discussion of different evolutionary

channels predicted by our model and estimate the fraction of magnetic and non-magnetic white dwarfs in CVs taking into account important parameters for binary star evolution^{44,73–76} as well as potential accretion heating and chemical impurities of the core of the white dwarf^{77–79}. We also elaborate on the implications of our scenario for the generation of magnetic fields in hot single white dwarfs⁸⁰ as well as magnetic white dwarfs in wide binaries⁸¹. We find that these magnetic fields are most likely generated by alternative mechanisms such as fossil fields resulting from main sequence star mergers^{82,83}, double white dwarf mergers¹⁹, or common envelope mergers^{18,84,85}.

Correspondence Correspondence and requests for materials should be addressed to M.R.S.

(email: matthias.schreiber@usm.cl).

Acknowledgements We thank the referee Chris Tout and two anonymous referees for their helpful comments. M.R.S. acknowledges support from the Millennium Nucleus for Planet Formation (NPF) and Fondecyt (grant 1181404). D.B. was supported by the grant #2017/14289-3, São Paulo Research Foundation (FAPESP) and ESO/Gobierno de Chile. B.T.G. was supported by the UK STFC grant ST/P000495. S.G.P. acknowledges the support of a STFC Ernest Rutherford Fellowship. M.Z. acknowledges support from CONICYT PAI (Concurso Nacional de Inserción en la Academia 2017, Folio 79170121) and CONICYT/FONDECYT (Programa de Iniciación, Folio 11170559)

Author contributions All authors contributed to the discussion and writing of this article. M.R.S. and D.B. developed the idea and carried out the simulations. S.G.P. and B.T.G. provided an observational overview of magnetic white dwarfs and recent observations of pre-polars. M.Z. provided crystallization temperatures for different white dwarf masses based on published white dwarf evolutionary sequences and estimated relative numbers of magnetic and non-magnetic CVs using binary population models.

Competing Interests The authors declare that they have no competing interests.

Data availability The data presented in this work is available upon request. In addition, the MESA files required to reproduce our simulations will be publicly available at the MESA Zenodo community (<https://zenodo.org/communities/mesa/>).

Code availability MESA is publicly available (<http://mesa.sourceforge.net/>).

Supplementary Discussion and Figures

The fraction of magnetic white dwarfs in CVs. We have shown that a crystallization and rotation driven dynamo can explain the properties of all close and strongly magnetic white dwarf binaries and the absence of magnetic white dwarfs in young detached white dwarf binary stars. In what follows we discuss under which conditions our model is likely to also reproduce the observed fraction of strongly magnetic white dwarfs in CVs. The measured fraction of strongly magnetic white dwarfs in CVs is more than one third (15 out of 42 systems within 150 pc^1). If the briefly detached pre-polars and AR Sco are included in this sample (the four pre-polars SDSS 0303+0054, WXLMi, SDSS J1212+0136, SDSS J1452+2045 and AR Sco are within $150 \text{ pc}^{3,10}$), the fraction of systems with magnetic white dwarfs further increases to 20 of 47 systems corresponding to 43 ± 6 per cent.

At first glance, our model might seem to produce too many magnetic white dwarfs in CVs as every white dwarf in a non-magnetic CV accretes angular momentum and is therefore expected to become rapidly rotating in a short period of time. In addition, if the white dwarf continuously cools it should start to crystallize and one might expect that our model predicts every white dwarf in a CV to eventually develop a strong magnetic field. However, accretion can increase the core temperature of white dwarfs in CVs⁷⁷ and prevent or delay crystallization. In addition, the generation of a strong magnetic field through the rotational and crystallization driven dynamo only works if fast rotation and a crystallizing core with an outer convection zone are present at the same time. The strength of the magnetic field generated by this dynamo depends on the convective energy flux² and most

likely also on the magnetic Prandtl number. However, in the absence of a scaling relation including the dependence on the latter, it remains unclear at which stages of crystallization the conditions are suitable for generating strong magnetic fields. In our model we assumed that in addition to fast rotation at least 10 per cent and not more than 80 per cent of the core need to be crystallized for the dynamo to be able to generate a strong magnetic field but this assumption is rather arbitrary. In what follows we describe the three different types of CVs that are non-magnetic according to our model and explain how the critical core mass ratios and other important parameters impact the predicted relative numbers of magnetic and non-magnetic CVs.

First (channel 1), our model predicts the white dwarfs in CVs that did not yet accrete enough angular momentum remain non-magnetic. How long this phase takes, and therefore also the relative number of CVs that are expected to be found in this stage in observed samples, depends on the efficiency of the accretion of angular momentum and the mass transfer rate (see equation 1 in the main text) which in turn depends on the angular momentum loss. For instance, CVs born with fully convective secondaries are expected to be driven by gravitational radiation only and typically have mass transfer rates 1-2 orders of magnitude lower than systems with earlier secondary stars. Therefore, the white dwarfs born with fully convective secondary stars will take longer to spin up to near-break velocities than those with earlier secondary stars that start mass transfer at longer orbital periods. However, as the spin up time scale is in general short compared to the secular time scale of CVs, we expect binary population synthesis based on our model to predict rather few CVs to be in this non-magnetic CV state.

Second (channel 2), CVs with white dwarfs that did not yet start the crystallization process in their cores remain non-magnetic CVs until the required condition is reached. How long this takes determines how many of such systems are predicted to exist in observed samples and depends on the fraction of crystallized core-mass that is assumed to be necessary to make the dynamo work (we assumed 10 per cent), on the time it takes the system to evolve from the common envelope to the CV phase, and whether accretion can heat up the core^{77,78} to avoid or delay crystallization. Assuming core heating is inefficient, according to recent white dwarf models²⁴ the time needed for a 0.6, 0.8 and 1.0 M_{\odot} white dwarf to have 10 per cent of its interior crystallized is approximately 3.2, 1.9 and 1.1 Gyr. This time span might be substantially increased for smaller white dwarf masses as the magnetic field needs to diffuse through a radiative zone which sits on top of the convective mantle. Only for massive white dwarfs the convective mantle extends close to the surface²⁰. This implies that detached binaries that emerged from common envelope evolution with short orbital periods, i.e. close to the start of mass transfer, can remain non-magnetic CVs for $\gtrsim 3$ Gyr. If core heating due to accretion is efficient and prevents the white dwarf from crystallizing during the CV phase, these CVs will even remain non-magnetic forever. Therefore a non-negligible number of non-magnetic CVs descending from short period post common envelope binaries is predicted to exist in observed samples of CVs.

Finally (channel 3), CVs containing white dwarfs that significantly crystallized before being spun up to fast rotation due to accretion, will not develop a strong magnetic field. In other words, if the white dwarf had enough time too cool so that a large fraction of its core is crystallized before the secondary fills its Roche-lobe, the convective energy flux in the outer core will not be sufficient

to generate a strong magnetic field. These systems will remain non-magnetic forever under the assumption that core heating due to accretion is inefficient. Even if accretion heating can melt a significant fraction of the core, this process is supposed to take several Gyr⁷⁸, i.e. the system would remain non-magnetic for a large fraction of its CV lifetime. Thus, whether a given system becomes a non-magnetic CV formed through this channel depends mostly on the time it spends between the white dwarf formation, i.e. the common envelope phase, and the onset of accretion. How many systems of a predicted CV population spend enough time in this detached white dwarf binary phase depends sensitively on the crystallized mass fraction (we assumed 80 per cent) at which the dynamo becomes unable to generate a strong magnetic field, on the inter-correlated initial orbital period, mass ratio, and eccentricity distributions of the progenitor systems, on the common envelope efficiency, and on the strength of angular momentum loss due to magnetic braking.

While the relative number of non-magnetic CVs predicted by our model through channel 1 is most likely very small, we expect that the other two groups of systems can easily explain the $\sim 50 - 70$ per cent of non-magnetic systems in the observed CV sample. Which of the two scenarios contributes more to the fraction of non-magnetic CVs depends on several assumptions. For example, for a large common envelope efficiency, relatively inefficient magnetic braking, and a critical crystallized mass fraction below 80 per cent, the majority of systems will evolve through channel 3 and will remain non-magnetic for at least several Gyr. In contrast, for a small common envelope efficiency, efficient magnetic braking, a large value for the critical fraction of crystallized core mass, and inefficient core heating, most CVs will eventually become magnetic but many of them may spend several Gyr as non-magnetic systems before the dynamo starts operating (channel

2).

The parameters (strengths of magnetic braking, critical crystallized mass fractions, common envelope efficiency, efficiency of core heating) are essential for predicting the evolution of close white dwarf binaries and for determining the fraction of strongly magnetic CVs predicted by our model. Unfortunately, several of these parameters are currently neither theoretically nor observationally well constrained. The common envelope efficiency is most likely relatively small as indicated by observational surveys of detached white dwarf binaries⁷³ and heating of the core is likely to play an important role^{77,78}. In contrast, the strength of magnetic braking is unknown⁶ and the same is true for the critical mass fractions (as detailed simulations for the dynamo we propose here do not yet exist). In addition, the initial binary parameter distributions usually assumed in CV population models are uncorrelated which is inconsistent with observational surveys performed in the past decades⁷⁶. These surveys show that the orbital period, primary mass, mass ratio and eccentricity distributions are inter-correlated. This is important because the combination of these parameters determines whether a given binary system will survive or not the common-envelope phase and which of those that survive and become CVs within the Hubble time, have relatively long or short detached lifetimes (possibly becoming slightly or highly crystallized) before the onset of mass transfer.

Based on binary population models we performed in the past^{74,75}, using standard parameters for CV evolution (common envelope efficiency of 0.25, magnetic braking according to Rappaport et al.⁴⁴, assuming the critical crystallized mass fractions used in this paper (i.e. 10 and 80 per cent),

and ignoring core heating of the white dwarf through accretion, we estimate the predicted fraction of magnetic systems to be roughly 50 per cent. While this value slightly exceeds the currently observed number of magnetic CVs, relatively small changes in the prescription for magnetic braking and/or the critical mass fractions of crystallized matter in the core of the white dwarf can easily bring into agreement the observed fractions and the predictions of our model. For the same assumptions but including efficient core heating, the predicted fraction of magnetic CVs decreases to ~ 20 per cent. This estimate is below the measured fraction but our conclusion remains unchanged as relatively small changes in uncertain parameters such as critical core mass and magnetic braking could increase the number of magnetic systems to match the observed fraction.

For the sake of completeness, as an additional unknown parameter, we emphasize that also the metallicity of the white dwarf progenitor star could play a role since the settling of neutronized impurities like ^{22}Ne and ^{56}Fe caused by solidification can release more energy than the separation of the C/O mixture which significantly affects the cooling of the white dwarf and the crystallization process⁷⁹.

As a final remark, we state that the small number of observationally discovered pre-polars and the even smaller number of AR Sco-like systems are in agreement with the relatively short time scale that our model predicts for these systems.

Implications for single white dwarfs and white dwarfs in wide binaries. The model presented in this paper describes a new evolutionary sequence for close white dwarf binaries which explains the origin and the relative numbers of strongly magnetic white dwarfs in these systems. While

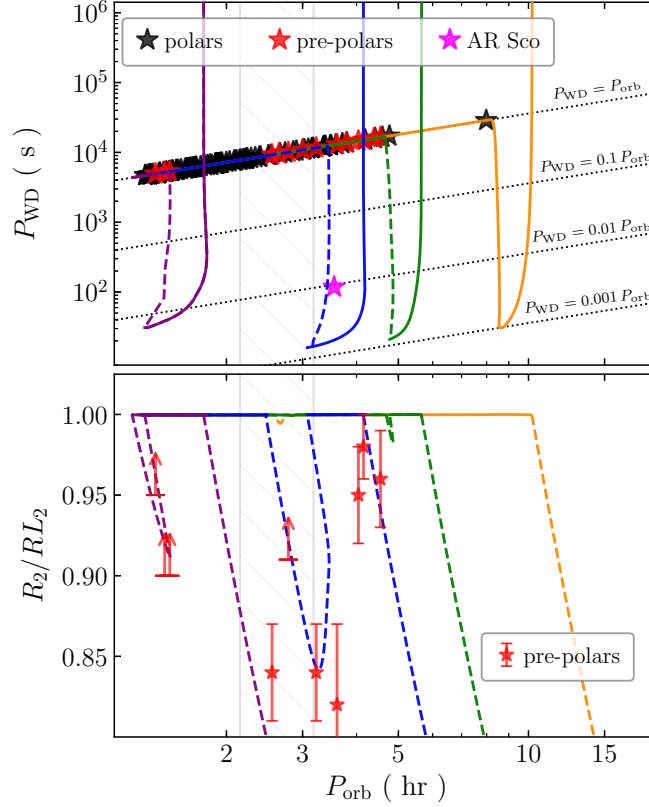
solving the puzzle for the occurrence of strongly magnetic white dwarfs in close binaries represents a key result on its own, we here briefly mention the implications for single white dwarfs and white dwarfs in wide binary stars.

It is clear that the dynamo proposed here to operate in CVs cannot explain all strongly magnetic single white dwarfs because it requires fast rotation and crystallization. A non-negligible number of strongly magnetic single white dwarfs⁷ are hot and therefore most likely not in the process of crystallization and, even worse, several of the highest field single white dwarfs are known to have rather long spin periods^{7, 80}. While field strengths of the order of 0.1 – 1 MG might be generated in crystallizing single white dwarfs with rotation periods of the order of hours or days, strong magnetic fields in single white dwarfs must be generated at least partly by a different mechanism. The same conclusion holds for the recently discovered strongly magnetic white dwarfs in wide binaries⁸¹. In most cases the separation between the two stars in these binaries exceeds several hundred astronomical units and therefore a previous phase of mass transfer and spin-up of the white dwarf can be excluded.

Similarly, the main mechanism for generating these strong magnetic fields in young single white dwarfs and wide binary stars must not be operating in close binaries as we would otherwise observe strongly magnetic white dwarfs in young detached close white dwarf binaries. The candidate scenarios that may fulfill this conditions are white dwarf mergers¹⁹, fossil fields¹⁷, or the common envelope merger scenario^{18,84,85}. Given that the most likely progenitors of magnetic white dwarfs according to the fossil field scenario are main sequence star mergers^{82,83}, all three

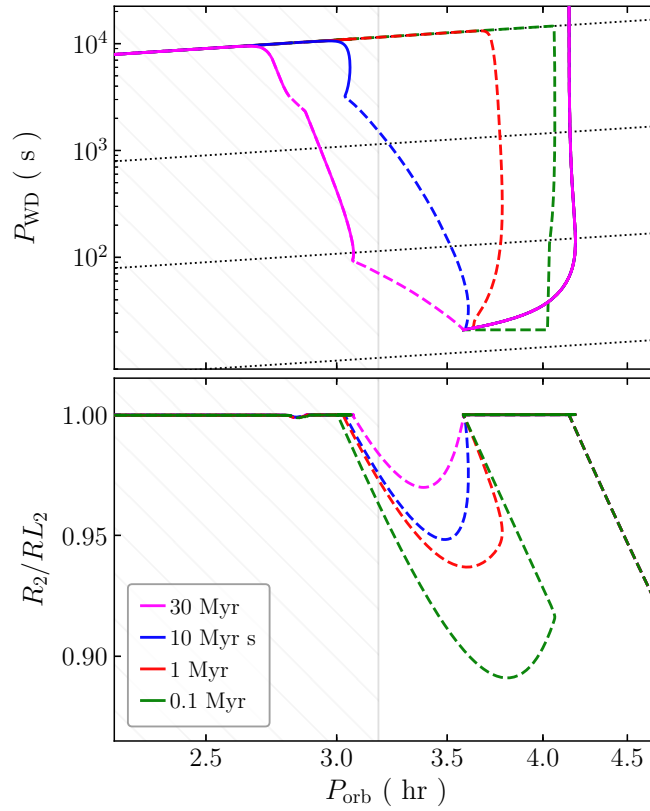
scenarios require single magnetic white dwarfs to form from binary stars. This implies that all scenarios require initial triple star configurations to produce strongly magnetic white dwarfs in binaries. As triples are intrinsically less common than binary stars, all three models may produce more strongly magnetic single white dwarfs than strongly magnetic white dwarfs in close and wide binaries. Which of the mechanisms is most suitable to explain magnetic single white dwarfs and magnetic white dwarfs in wide binaries depends on the relatively poorly constraint distribution of initial triple star configurations.

We conclude that the crystallization and rotation driven dynamo proposed here explains the large number of magnetic white dwarfs in CVs, as well as the existence and characteristics of AR Sco and the pre-polars, and might be complemented by e.g. the double white dwarf merger and/or the common envelope merger scenario which are good candidates for explaining strongly magnetic single white dwarfs.

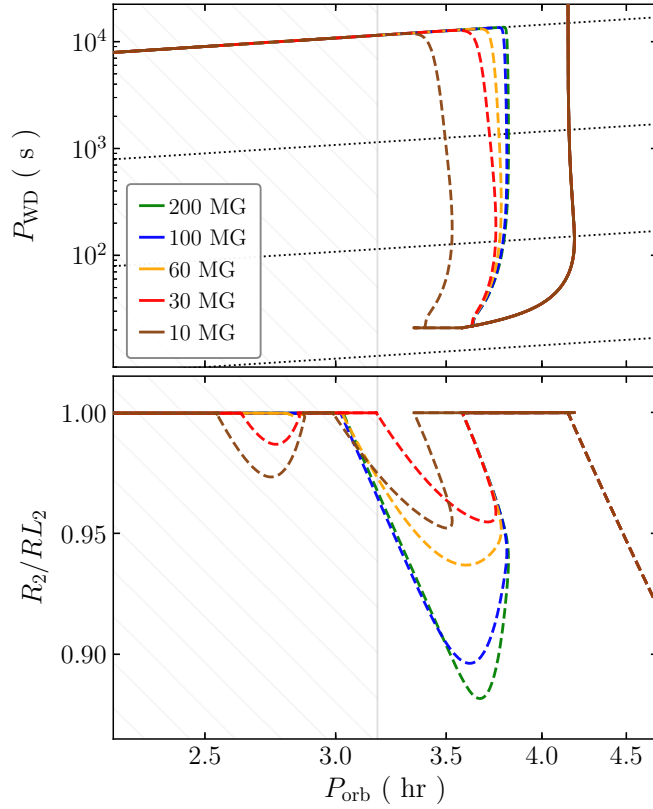


Supplementary Figure 1. Comparison of different evolutionary tracks with observations. The detached phases (dashed lines) explain the existence of only cool magnetic white dwarfs in detached binaries that are close to Roche-lobe filling because the magnetic field was generated during the CV phase when the white dwarf was old and crystallizing. The model also offers an explanation for AR Sco which in fact is a progenitor of the pre-polars. In AR Sco, nicely reproduced by the blue track, the secondary detached from its Roche-lobe but spin and orbital motion are not yet synchronised. The subsequent detached synchronised phase explains the orbital periods, Roche-lobe filling factors, and white dwarf temperatures of pre-polars. To generate the tracks we only changed the initial orbital period (P_i) and initial secondary mass (M_2), as well as the white dwarf spin period (P_{WD}) when the magnetic field is generated. The parameters we used were the fol-

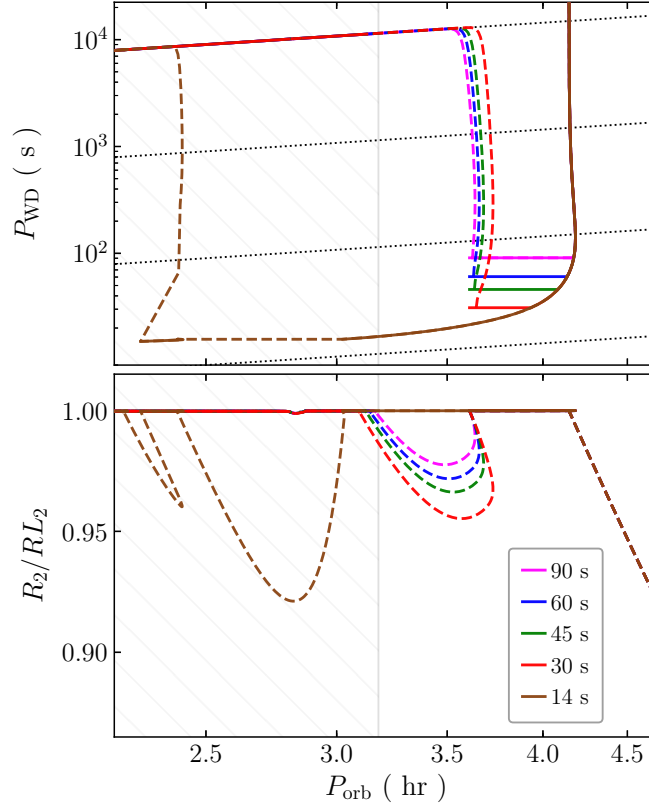
lowing $P_i = 0.14$ days, $M_2 = 0.17 M_\odot$, $P_{\text{WD}} = 30$ s (purple), $P_i = 0.68$ days, $M_2 = 0.55 M_\odot$, $P_{\text{WD}} = 15$ s (blue), $P_i = 0.925$ days, $M_2 = 0.75 M_\odot$, $P_{\text{WD}} = 20$ s (green), $P_i = 1.544$ days, $M_2 = 1.2 M_\odot$, $P_{\text{WD}} = 30$ s (orange). In all tracks the white dwarf mass was assumed to be $0.8 M_\odot$ ²⁹ and the generated magnetic field strengths was assumed to be 60 MG. The errorbars on the observations correspond to 1σ .



Supplementary Figure 2. Evolutionary sequences highlighting the impact of different choices of the synchronisation time scale. The shorter the time scale, the more pronounced and the longer the detached phase. For the longest time scales (blue, purple), accretion starts before the system synchronised. Time scales exceeding 1 Myr are most likely not realistic.



Supplementary Figure 3. Evolutionary sequences highlighting the impact of the white dwarf magnetic field strength. The stronger the generated field, the longer the detached phase as angular momentum loss due to magnetic braking is more reduced. For the weakest field strengths (brown, red), a less pronounced standard gap still occurs when the secondary becomes fully convective.



Supplementary Figure 4. Evolutionary sequences highlighting the impact of different choices of the white dwarf spin period (P_{WD}) at onset of magnetic field generation. The hatched region indicates the locus of the standard orbital period gap. In each track, solid and dashed lines correspond to semi-detached and detached phases respectively. With the exception of the case $P_{\text{WD}} = 14$ s (brown curve), a detached phase is generated above the standard orbital period gap, at an orbital period ≈ 3.75 hr. For P_{WD} at least twice the break-up period, magnetic field generation starts at the same period and the slower the spin, the shorter the detached phase. To spin-up the white dwarf to velocities close to the break-up period (brown track), the spin-up phase is much longer and therefore the pronounced detached phase occurs at a significantly shorter orbital period.

1. Pala, A. F. *et al.* A Volume-limited Sample of Cataclysmic Variables from Gaia DR2: Space Density and Population Properties. *Mon. Not. R. Astron. Soc.* **494**, 3799–3827 (2020).
2. Christensen, U. R., Holzwarth, V. & Reiners, A. Energy flux determines magnetic field strength of planets and stars. *Nature* **457**, 167–169 (2009).
3. Marsh, T. R. *et al.* A radio-pulsing white dwarf binary star. *Nature* **537**, 374–377 (2016).
4. Ivanova, N. *et al.* Common envelope evolution: where we stand and how we can move forward. *Astron. Astrophys. Rev.* **21**, 59 (2013).
5. Schreiber, M. R. & Gänsicke, B. T. The age, life expectancy, and space density of Post Common Envelope Binaries. *Astron. Astrophys.* **406**, 305–321 (2003).
6. Knigge, C., Baraffe, I. & Patterson, J. The Evolution of Cataclysmic Variables as Revealed by Their Donor Stars. *Astrophys. J. Suppl.* **194**, 28 (2011).
7. Ferrario, L., de Martino, D. & Gänsicke, B. T. Magnetic White Dwarfs. *Space Sci. Rev.* **191**, 111–169 (2015).
8. Norton, A. J., Wynn, G. A. & Somerscales, R. V. The Spin Periods and Magnetic Moments of White Dwarfs in Magnetic Cataclysmic Variables. *Astrophys. J.* **614**, 349–357 (2004).
9. Schwobe, A. D., Nebot Gomez-Moran, A., Schreiber, M. R. & Gänsicke, B. T. Post common envelope binaries from the SDSS. VI. SDSS J120615.73+510047.0: a new low accretion rate magnetic binary. *Astron. Astrophys.* **500**, 867–872 (2009).

10. Parsons, S. G. *et al.* Magnetic white dwarfs in post-common-envelope binaries. *Mon. Not. R. Astron. Soc.* **in press**, arXiv:2101.08792 (2021).
11. Schreiber, M. R. *et al.* Post common envelope binaries from SDSS. VIII. Evidence for disrupted magnetic braking. *Astron. Astrophys.* **513**, L7 (2010).
12. Rebassa-Mansergas, A. *et al.* Post-common envelope binaries from SDSS - XIV. The DR7 white dwarf-main-sequence binary catalogue. *Mon. Not. R. Astron. Soc.* **419**, 806–816 (2012).
13. Reimers, D., Hagen, H. J. & Hopp, U. HS 1023+3900 - a magnetic CV in the period gap with a distinct cyclotron emission line spectrum. *Astron. Astrophys.* **343**, 157–162 (1999).
14. Schmidt, G. D. *et al.* New Low Accretion Rate Magnetic Binary Systems and their Significance for the Evolution of Cataclysmic Variables. *Astrophys. J.* **630**, 1037–1053 (2005).
15. Liebert, J. *et al.* Where Are the Magnetic White Dwarfs with Detached, Nondegenerate Companions? *Astron. J.* **129**, 2376–2381 (2005).
16. Belloni, D. & Schreiber, M. R. Are white dwarf magnetic fields in close binaries generated during common-envelope evolution? *Mon. Not. R. Astron. Soc.* **492**, 1523–1529 (2020).
17. Braithwaite, J. & Spruit, H. C. A fossil origin for the magnetic field in A stars and white dwarfs. *Nature* **431**, 819–821 (2004).
18. Tout, C. A., Wickramasinghe, D. T., Liebert, J., Ferrario, L. & Pringle, J. E. Binary star origin of high field magnetic white dwarfs. *Mon. Not. R. Astron. Soc.* **387**, 897–901 (2008).

19. García-Berro, E. *et al.* Double Degenerate Mergers as Progenitors of High-field Magnetic White Dwarfs. *Astrophys. J.* **749**, 25 (2012).
20. Isern, J., García-Berro, E., Külebi, B. & Lorén-Aguilar, P. A Common Origin of Magnetism from Planets to White Dwarfs. *Astrophys. J. Lett.* **836**, L28 (2017).
21. Lister, J. R. & Buffett, B. A. The strength and efficiency of thermal and compositional convection in the geodynamo. *Physics of the Earth and Planetary Interiors* **91**, 17–30 (1995).
22. Paxton, B. *et al.* Modules for Experiments in Stellar Astrophysics (MESA): Pulsating Variable Stars, Rotation, Convective Boundaries, and Energy Conservation. *Astrophys. J. Suppl.* **243**, 10 (2019).
23. King, A. R., Regev, O. & Wynn, G. A. Evolution of the white dwarf mass and spin in cataclysmic variables. *Mon. Not. R. Astron. Soc.* **251**, 30P–32P (1991).
24. Bédard, A., Bergeron, P., Brassard, P. & Fontaine, G. On the Spectral Evolution of Hot White Dwarf Stars. I. A Detailed Model Atmosphere Analysis of Hot White Dwarfs from SDSS DR12. *Astrophys. J.* **901**, 93 (2020).
25. Belloni, D. *et al.* Evidence for reduced magnetic braking in polars from binary population models. *Mon. Not. R. Astron. Soc.* **491**, 5717–5731 (2020).
26. Hameury, J. M., King, A. R., Lasota, J. P. & Ritter, H. The Evolution of Magnetic Cataclysmic Variables. *Astrophys. J.* **316**, 275 (1987).

27. Nebot Gómez-Morán, A. *et al.* Post common envelope binaries from SDSS. XII. The orbital period distribution. *Astron. Astrophys.* **536**, A43 (2011).
28. Garnavich, P., Littlefield, C., Lyutikov, M. & Barkov, M. Peeking Between the Pulses: The Far-UV Spectrum of the Previously Unseen White Dwarf in AR Scorpii. *Astrophys. J.* **in press**, arXiv:2012.09868 (2021).
29. Zorotovic, M., Schreiber, M. R. & Gänsicke, B. T. Post common envelope binaries from SDSS. XI. The white dwarf mass distributions of CVs and pre-CVs. *Astron. Astrophys.* **536**, A42 (2011).
30. Schreiber, M. R., Zorotovic, M. & Wijnen, T. P. G. Three in one go: consequential angular momentum loss can solve major problems of CV evolution. *Mon. Not. R. Astron. Soc.* **455**, L16–L20 (2016).
31. Christensen, U. R. Dynamo Scaling Laws and Applications to the Planets. *Space Sci. Rev.* **152**, 565–590 (2010).
32. Christensen, U. R. & Aubert, J. Scaling properties of convection-driven dynamos in rotating spherical shells and application to planetary magnetic fields. *Geophysical Journal International* **166**, 97–114 (2006).
33. van Horn, H. M. Crystallization of White Dwarfs. *Astrophys. J.* **151**, 227 (1968).
34. Segretain, L. & Chabrier, G. Crystallization of binary ionic mixtures in dense stellar plasmas. *Astron. Astrophys.* **271**, L13 (1993).

35. Horowitz, C. J., Schneider, A. S. & Berry, D. K. Crystallization of Carbon-Oxygen Mixtures in White Dwarf Stars. *Phys. Rev. Lett.* **104**, 231101 (2010).
36. Isern, J., Mochkovitch, R., García-Berro, E. & Hernanz, M. The Physics of Crystallizing White Dwarfs. *Astrophys. J.* **485**, 308–312 (1997).
37. Isern, J., García-Berro, E., Hernanz, M. & Chabrier, G. The Energetics of Crystallizing White Dwarfs Revisited Again. *Astrophys. J.* **528**, 397–400 (2000).
38. Brandenburg, A. Magnetic Prandtl Number Dependence of the Kinetic-to-magnetic Dissipation Ratio. *Astrophys. J.* **791**, 12 (2014).
39. Campbell, C. G. The maintenance of corotation in the strong polars. *Mon. Not. R. Astron. Soc.* **215**, 509–516 (1985).
40. Campbell, C. G. Magnetospherically induced torques in asynchronous AMHerculis binaries. *Mon. Not. R. Astron. Soc.* **409**, 433–446 (2010).
41. Mestel, L. Magnetic braking by a stellar wind-I. *Mon. Not. R. Astron. Soc.* **138**, 359 (1968).
42. Webbink, R. F. & Wickramasinghe, D. T. Cataclysmic variable evolution: AM Her binaries and the period gap. *Mon. Not. R. Astron. Soc.* **335**, 1–9 (2002).
43. Li, J. K., Wu, K. W. & Wickramasinghe, D. T. Reduced Magnetic Braking in Synchronously Rotating Magnetic Cataclysmic Variables. *Mon. Not. R. Astron. Soc.* **268**, 61 (1994).
44. Rappaport, S., Verbunt, F. & Joss, P. C. A new technique for calculations of binary stellar evolution, with application to magnetic braking. *Astrophys. J.* **275**, 713–731 (1983).

45. Paxton, B. *et al.* Modules for Experiments in Stellar Astrophysics (MESA). *Astrophys. J. Suppl.* **192**, 3 (2011).
46. Paxton, B. *et al.* Modules for Experiments in Stellar Astrophysics (MESA): Planets, Oscillations, Rotation, and Massive Stars. *Astrophys. J. Suppl.* **208**, 4 (2013).
47. Paxton, B. *et al.* Modules for Experiments in Stellar Astrophysics (MESA): Binaries, Pulsations, and Explosions. *Astrophys. J. Suppl.* **220**, 15 (2015).
48. Paxton, B. *et al.* Modules for Experiments in Stellar Astrophysics (MESA): Convective Boundaries, Element Diffusion, and Massive Star Explosions. *Astrophys. J. Suppl.* **234**, 34 (2018).
49. Rogers, F. J. & Nayfonov, A. Updated and Expanded OPAL Equation-of-State Tables: Implications for Helioseismology. *Astrophys. J.* **576**, 1064–1074 (2002).
50. Saumon, D., Chabrier, G. & van Horn, H. M. An Equation of State for Low-Mass Stars and Giant Planets. *Astrophys. J. Suppl.* **99**, 713 (1995).
51. Pols, O. R., Tout, C. A., Eggleton, P. P. & Han, Z. Approximate input physics for stellar modelling. *Mon. Not. R. Astron. Soc.* **274**, 964–974 (1995).
52. Timmes, F. X. & Swesty, F. D. The Accuracy, Consistency, and Speed of an Electron-Positron Equation of State Based on Table Interpolation of the Helmholtz Free Energy. *Astrophys. J. Suppl.* **126**, 501–516 (2000).

53. Potekhin, A. Y. & Chabrier, G. Thermodynamic Functions of Dense Plasmas: Analytic Approximations for Astrophysical Applications. *Contributions to Plasma Physics* **50**, 82–87 (2010).
54. Iglesias, C. A. & Rogers, F. J. Radiative opacities for carbon- and oxygen-rich mixtures. *Astrophys. J.* **412**, 752–760 (1993).
55. Iglesias, C. A. & Rogers, F. J. Updated Opal Opacities. *Astrophys. J.* **464**, 943 (1996).
56. Ferguson, J. W. *et al.* Low-Temperature Opacities. *Astrophys. J.* **623**, 585–596 (2005).
57. Buchler, J. R. & Yueh, W. R. Compton scattering opacities in a partially degenerate electron plasma at high temperatures. *Astrophys. J.* **210**, 440–446 (1976).
58. Cassisi, S., Potekhin, A. Y., Pietrinferni, A., Catelan, M. & Salaris, M. Updated Electron-Conduction Opacities: The Impact on Low-Mass Stellar Models. *Astrophys. J.* **661**, 1094–1104 (2007).
59. Angulo, C. *et al.* A compilation of charged-particle induced thermonuclear reaction rates. *Nucl. Phys. A* **656**, 3–183 (1999).
60. Cyburt, R. H. *et al.* The JINA REACLIB Database: Its Recent Updates and Impact on Type-I X-ray Bursts. *Astrophys. J. Suppl.* **189**, 240–252 (2010).
61. Fuller, G. M., Fowler, W. A. & Newman, M. J. Stellar weak interaction rates for intermediate-mass nuclei. IV - Interpolation procedures for rapidly varying lepton capture rates using effective $\log(\text{ft})$ -values. *Astrophys. J.* **293**, 1–16 (1985).

62. Oda, T., Hino, M., Muto, K., Takahara, M. & Sato, K. Rate Tables for the Weak Processes of sd-Shell Nuclei in Stellar Matter. *Atomic Data and Nuclear Data Tables* **56**, 231–403 (1994).
63. Langanke, K. & Martínez-Pinedo, G. Shell-model calculations of stellar weak interaction rates: II. Weak rates for nuclei in the mass range $A=45-65$ in supernovae environments. *Nuclear Physics A* **673**, 481–508 (2000).
64. Chugunov, A. I., Dewitt, H. E. & Yakovlev, D. G. Coulomb tunneling for fusion reactions in dense matter: Path integral MonteCarlo versus mean field. *Phys. Rev. D* **76**, 025028 (2007).
65. Itoh, N., Hayashi, H., Nishikawa, A. & Kohyama, Y. Neutrino Energy Loss in Stellar Interiors. VII. Pair, Photo-, Plasma, Bremsstrahlung, and Recombination Neutrino Processes. *Astrophys. J. Suppl.* **102**, 411 (1996).
66. Eggleton, P. P. Approximations to the radii of Roche lobes. *Astrophys. J.* **268**, 368 (1983).
67. Ritter, H. Turning on and off mass transfer in cataclysmic binaries. *Astron. Astrophys.* **202**, 93–100 (1988).
68. Matthews, J. H., Knigge, C., Long, K. S., Sim, S. A. & Higginbottom, N. The impact of accretion disc winds on the optical spectra of cataclysmic variables. *Mon. Not. R. Astron. Soc.* **450**, 3331–3344 (2015).
69. Coppejans, D. L. & Knigge, C. The case for jets in cataclysmic variables. *New Astronomy Reviews* **89**, 101540 (2020).

70. Reiners, A. & Basri, G. The First Direct Measurements of Surface Magnetic Fields on Very Low Mass Stars. *Astrophys. J.* **656**, 1121–1135 (2007).
71. McAllister, M. *et al.* The evolutionary status of Cataclysmic Variables: eclipse modelling of 15 systems. *Mon. Not. R. Astron. Soc.* **486**, 5535–5551 (2019).
72. Stiller, R. A. *et al.* High-time-resolution Photometry of AR Scorpii: Confirmation of the White Dwarf’s Spin-down. *Astron. J.* **156**, 150 (2018).
73. Zorotovic, M., Schreiber, M. R., Gänsicke, B. T. & Nebot Gómez-Morán, A. Post-common-envelope binaries from SDSS. IX: Constraining the common-envelope efficiency. *Astron. Astrophys.* **520**, A86 (2010).
74. Zorotovic, M. *et al.* Monte Carlo simulations of post-common-envelope white dwarf + main sequence binaries: The effects of including recombination energy. *Astron. Astrophys.* **568**, A68 (2014).
75. Belloni, D. *et al.* No cataclysmic variables missing: higher merger rate brings into agreement observed and predicted space densities. *Mon. Not. R. Astron. Soc.* **478**, 5626–5637 (2018).
76. Moe, M. & Di Stefano, R. Mind Your Ps and Qs: The Interrelation between Period (P) and Mass-ratio (Q) Distributions of Binary Stars. *Astrophys. J. Suppl.* **230**, 15 (2017).
77. Townsley, D. M. & Bildsten, L. Theoretical Modeling of the Thermal State of Accreting White Dwarfs Undergoing Classical Nova Cycles. *Astrophys. J.* **600**, 390–403 (2004).

78. Epelstain, N., Yaron, O., Kovetz, A. & Prialnik, D. A thousand and one nova outbursts. *Mon. Not. R. Astron. Soc.* **374**, 1449–1456 (2007).
79. Isern, J., García-Berro, E., Hernanz, M. & Mochkovitch, R. The physics of white dwarfs. *Journal of Physics Condensed Matter* **10**, 11263–11272 (1998).
80. Charpinet, S., Fontaine, G. & Brassard, P. Seismic evidence for the loss of stellar angular momentum before the white-dwarf stage. *Nature* **461**, 501–503 (2009).
81. Landstreet, J. D. & Bagnulo, S. Discovery of a Sirius-like binary system with a very strongly magnetic white dwarf. Binarity among magnetic white dwarfs. *Astron. Astrophys.* **634**, L10 (2020).
82. Ferrario, L., Pringle, J. E., Tout, C. A. & Wickramasinghe, D. T. The origin of magnetism on the upper main sequence. *Mon. Not. R. Astron. Soc.* **400**, L71–L74 (2009).
83. Schneider, F. R. N. *et al.* Stellar mergers as the origin of magnetic massive stars. *Nature* **574**, 211–214 (2019).
84. Wickramasinghe, D. T., Tout, C. A. & Ferrario, L. The most magnetic stars. *Mon. Not. R. Astron. Soc.* **437**, 675–681 (2014).
85. Briggs, G. P., Ferrario, L., Tout, C. A., Wickramasinghe, D. T. & Hurley, J. R. Merging binary stars and the magnetic white dwarfs. *Mon. Not. R. Astron. Soc.* **447**, 1713–1723 (2015).